NUMERICAL INVESTIGATION OF THE FLOW INSIDE PRIMARY ZONE OF TUBULAR COMBUSTOR MODEL

Yehia A. Eldrainy, Mohammad Nazri Mohd Jaafar[*], Tholudin Mat Lazim

Aeronautical Engineering Department
Faculty of Mechanical Engineering
Universiti Teknologi Malaysia

ABSTRACT

In this study, a numerical simulation of non-reacting flow inside a gas turbine combustor model was performed. The main target of this investigation is to get physical insight of the main vortex, responsible for the efficient mixing of fuel and air. Such models are necessary for developing and optimization of real combustors. Combustor swirler assists the fuel-air mixing process by producing recirculation region which can act as flame holders as well. Therefore, proper selection of a swirler is needed to stabilize the flame, to enhance combustor performance and to reduce NOx emissions. For that reason, several axial swirlers with different configurations were employed to show their effects on primary zone aerodynamics performance. The three-dimensional, steady, turbulent and isothermal flow inside the combustor model was simulated using a finite volume based CFD code FLUENT 6.2. The combustor model geometry was created by means of solid model CAD software then the meshing was generated using GAMBIT preprocessing software subsequently, and the solution and the results analysis were carried out in a FLUENT solver. The effects of different swirlers' configurations and inlet mass flow rate on flow dynamics were examined. A two recirculation zones were predicted, the first one is a central recirculation and located in the region immediately downstream of the swirler and the second is corner recirculation and located in the upstream corner of the combustion chamber. The results show that swirlers' configuration and inlet mass flow rate have a significant effect on the combustor flowfield and pressure losses. By the mean that as swirl number increases the central recirculation zone size, turbulence production and pressure loss increase.

Keywords: *Isothermal flow, numerical simulation, tubular combustor, turbulence, air swirler*

1.0   INTRODUCTION

In combustors of aero and industry gas turbines, producing strong swirl is essential to the combustion air in order to assist in flame stabilization of the high intensity combustion and low emission combustion. The degree of the swirl

---

[*] Corresponding author: E-mail: nazri@fkm.utm.my

applied to the flow affect the flame size, shape and stability as well as the combustion intensity. Swirl flows are characterized by swirl number S_N which is defined as the ratio between axial flux of the angular momentum to the axial momentum [1], [2], [3].

$$S_N = \frac{\int_0^R (wr)\rho u 2\pi r dr}{R\int_0^R u\rho u 2\pi r dr} \tag{1}$$

For an axial swirler having a uniform swirl angle, the swirl number is related to the swirl angle θ, inner radius r_i and outer radius r_o as given by [3]:

$$S_N = \frac{2}{3}\left[\frac{1-(r_i/r_o)^3}{1-(r_i/r_o)^2}\right]\tan\theta \tag{2}$$

At high degree of swirl ($S_N > 0.6$) strong radial and axial pressure gradients are generated near the swirler exit plane. The relation between pressure gradient $\frac{\partial p}{\partial r}$ and tangential velocity w can be written in the following form [4]:

$$\frac{\partial p}{\partial r} = \frac{\rho w^2}{r} \tag{3}$$

As the result of these pressure gradients, an axial recirculation zone is formed in the form of a central trapezoidal recirculation zone, CTRZ, which is not observed in low swirl number ($S_N < 0.4$). CRTZ plays a dominant role in flame stabilization by providing hot recirculated gases to the combustion zone and reduced velocity matching the low flame velocity. The mean axial Mach number leaving the primary zone must be of the order 0.02 to 0.05 [5]. Most swirlers are designed to produce swirl number in between 0.4 to 0.6 to ensure adequate recirculation for anchoring flame stability without excessive pressure loss [1].

In this study, three swirlers with different blade angles 30°, 45° and 60° which are corresponding to swirl number 0.43, 0.74, and 1.28 respectively were analyzed numerically at different inlet boundary conditions to show the effect of the swirler configuration on the turbulence production, recirculation zone as well as pressure loss.

Due the complexity of the flow within the gas turbine combustor, CFD is used as a regular tool to enable better understanding of the aerodynamic and process associated to combustion of the gas turbine combustion chambers. Nowadays CFD is employed in design and development of more efficient and low emission combustors.

Numerical simulation of the flow field within the gas turbine combustor mainly utilizes Reynolds Average Navier Stokes (RANS) methods accompanied with closure turbulent models. In this paper the turbulent Reynolds stresses and other turbulent flow quantities are predicted with the standard k-ε model in calculating

the isothermal flow in a model gas turbine combustor because of its robustness, economy, and reasonable accuracy for a wide range of turbulent flows [6].

Menzies [7] had studied the behavior of five k-ε variants in modeling the isothermal flow inside a gas turbine combustor and compared the numerical results with the experimental data of Da Palma [8] for the velocity and turbulence fields. The studied models were the standard, the RNG, the realizable, the Durbin modified, and the nonlinear k-ε models. The results showed that the standard and the Durbin k-ε models gave the best agreement with the experimental. The nonlinear k-ε model also gave acceptable results but with additional formulation complexity and convergence problems.

Hsiao and Mongia [9] studied the behavior of the standard k-ε, the realizable k-ε, the RNG k-ε, the standard k-ω, and the RSM models in simulating the flow inside a swirl cup combustor was assessed using LDV measurements. The shape of the central recirculation zone (CRZ) (Figure 2) predicted by the five models along with that measured by the LDV revealed the efficiency of the standard model in predicting this type of flow when compared to the other eddy viscosity models. For the axial velocity predictions, the RNG and k-ω models performed poorly in the central recirculation and near wall regions. The realizable and the RSM models did not predict velocity profiles in the wake recovery area well. On the other hand, the standard k-ε model results match very well with the experiment. For the turbulence kinetic energy prediction, upstream of the impingement point the standard k-ε gave the closest results to the experiment, followed by the realizable k-ε model. The other models failed to correctly predict the profiles of the turbulence kinetic energy. Downstream of the impingement point all the models showed less turbulent diffusion than the experiment. In the above computer experiments, the RNG model obtained a worse agreement with the experimental measurements than the standard model.

2.0   GOVERNING EQUATION

Three dimensional, incompressible steady state isothermal flow is assumed. Based on these assumptions, the Reynolds-averaged Navier-Stokes equations are:

$$\frac{\partial \overline{u}_i}{\partial x_i} = 0 \tag{4}$$

$$\overline{u}_j \frac{\partial \overline{u}_i}{\partial x_j} = -\frac{1}{\rho} \frac{\partial \overline{p}}{\partial x_i} + \nu \frac{\partial^2 \overline{u}_i}{\partial x_j \partial x_j} - \frac{\partial \overline{u_i' u_j'}}{\partial x_j} \tag{5}$$

Where $\overline{u}$ is the mean velocity component in x_i direction, ρ is the density, p is the mean pressure and ν is the kinematic viscosity. The overbar denotes time averaging, and the prime denotes fluctuating component.

3.0 TURBULENT MODELS

The main feature of the turbulent flow is the random fluctuations of fluid velocity over space and time. These random fluctuations occur over very small distances in space and time compared to the overall domain. In order for a turbulent flow to be resolved the computational mesh size must be smaller than the smallest element of turbulent motion (eddy). The computations have to be unsteady using a time-step smaller than that of the fastest eddy. This leads to an impossibly large number of grid nodes and time steps. The calculations required are beyond the capabilities of current computing technology.

As engineers are not usually interested in the fluctuating components of flow a statistical approach is taken. This is achieved by averaging over a time scale that is large compared with the turbulent motion. The results from these equations describe the flow in terms of the mean velocities and pressures. However, these equations contain unknowns representing the Reynolds stress and transport of mean momentum. These additional equations (turbulence modeling) are needed to be solved for all the parameters. The number of these additional equations increases with the complexity of the model. Basically, turbulent models incorporated with the governing equations are used to determine the Reynolds Stresses.

The k-ε model focuses on the mechanisms that affect the turbulent kinetic energy. The standard k-ε model in FLUENT falls within this class of turbulence model and has become the workhorse of practical engineering flow calculations in the time since it was proposed by Jones and Launder [10]. Robustness, economy, and reasonable accuracy for a wide range of turbulent flows explain its popularity in industrial flow and heat transfer simulations. It is a semi-empirical model, and the derivation of the model equations relies on phenomenological considerations and empiricism. As the strengths and weaknesses of the standard k-e model have become known, improvements have been made to the model to improve its performance.

Generally k-ε models solve two additional transport equations - one for the turbulent kinetic energy and the other is for the turbulent dissipation rate. These models uses Boussinesq hypothesis which proposes that the transport of momentum by turbulence is a diffusive process and thus the Reynolds stresses $(-\overline{u_i' u_j'})$ can be modelled using turbulent (eddy) viscosity which is analogous to molecular viscosity.

$$-\overline{u_i' u_j'} = 2\upsilon_t \left(\frac{\partial \overline{u}_i}{\partial x_j} + \frac{\partial \overline{u}_j}{\partial x_i} \right) - \frac{2}{3} k\, \delta_{ij} \tag{6}$$

4.0 COMPUTATIONAL METHOD

The swirling flow enters the domain from axial swirler (r_i = 9.5 mm, r_o=23.9) with different blade angles of 30°, 45° and 60° from the direction of inlet air flow. The flow expands into the combustion volume under an angle of 90 degrees i.e. the

diffuser is sudden expansion type. The downstream part (combustion chamber) of the flow domain is a cylinder with a radius of 72.5 mm and a length of 400 mm.

The model geometry had been created using solid model, and grids (Figure 1) of all the computational regions considered in this study were set up with preprocessing package GAMBIT version 2.2. Grid generation and density play an important role in the prediction of solution accuracy [11]. The grid was non-uniform, with high density in zones of great interest i.e. zones of high gradients and low density in zones of less interest, so that minimal computational effort was required whilst gaining sufficient accuracy.

In order to obtain a grid-independent solution, the grid should be refined until the solution no longer varies with additional grid refinement. The solution of the CFD models has been achieved using FLUENT 6.2 [12]. At the inlet of the computational region, the inlet boundary condition is defined as mass flow inlet while the exit boundary is defined as pressure outlet (gauge pressure at model outlet is 0.0). Some assumptions about boundary conditions that were not directly measured had to be made as follows:

- Velocity components and turbulence quantities at the inlet were constant
- Turbulence at inlet is calculated from the following equations [13]:

$$k_{inlet} = 0.002 (u^2)_{inlet} \tag{7}$$

$$\varepsilon = \frac{k_{inlet}^{1.5}}{0.3 D} \tag{8}$$

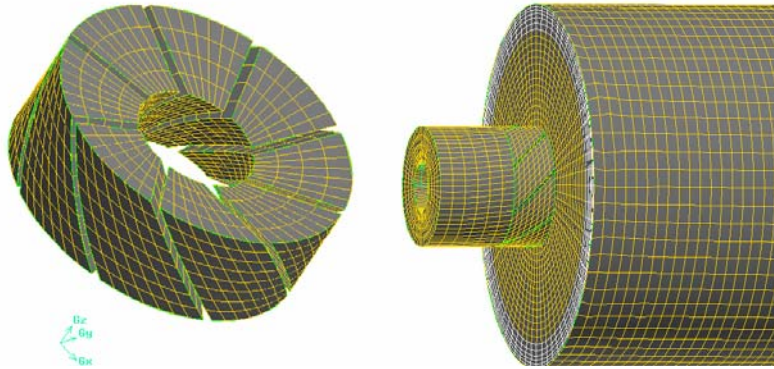Where u axial inlet flow velocity and *D* is hydraulic diameter

Figure 1: Computational gird of combustor

5.0   RESULTS AND DISCUSSION

Computations have been made to predict the capabilities of the code to simulate the flow field in non-premixed sudden expansion (dump) combustor. To study the effect of the inlet velocity, different swirler angles and number of the swirler blade

on the flow field of the combustor on isothermal flow conditions. Constant swirler root and tip diameters and blade thickness are assumed for all cases under study.

5.1   Mesh Refinement Study
In order to obtain a grid-independent solution, the grid should be refined until the solution no longer varies with additional grid. Grid refinement and density play an important role in the prediction of solution accuracy. The effect of Mesh refinement on the solution was investigated for mass flow for 0.16 kg/s and the meshes used are 175269, 284812 and 59243 respectively. Figure 2 shows the solution of the axial velocity along the centerline of the combustor. It can be seen that the solutions converge as the mesh refined. There is a good agreement of the axial velocity along the combustor centerline for 284812 and 59243 mesh sizes. Therefore, it can be concluded that mesh size 284812 provides a sufficiently grid-independent solutions.
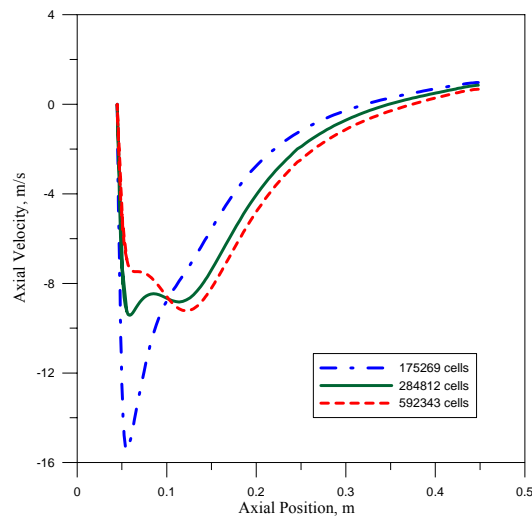
Figure 2: Axial velocity distributions at centerline for different meshes number

5.2   Recirculation Zone
One of the important features of the incoming flow into a combustor is the creation of the recirculation zones. The resulting flow field domain possesses a central recirculation zone around the centerline of combustor and downstream of the air swirler, in addition to a corner recirculation zone near the upper corner provoked by the sudden enlargement of the cross sectional area of the combustor. The two zones can be identified clearly in Figures 3 (a) and (b). Figure 4 shows that the axial velocity decays in the downstream direction. After stagnation point the reverse axial velocities disappear and the peak of the axial velocity profile shifts toward the centerline as the effect of the swirl diminishes. The recirculation zone in swirling flow is closely related to the inlet flow Reynolds number Re_D, swirl number S_N, and affected by the upstream and downstream boundary

conditions. So the effects of these factors on the swirling flow field will be investigated in the following sections.
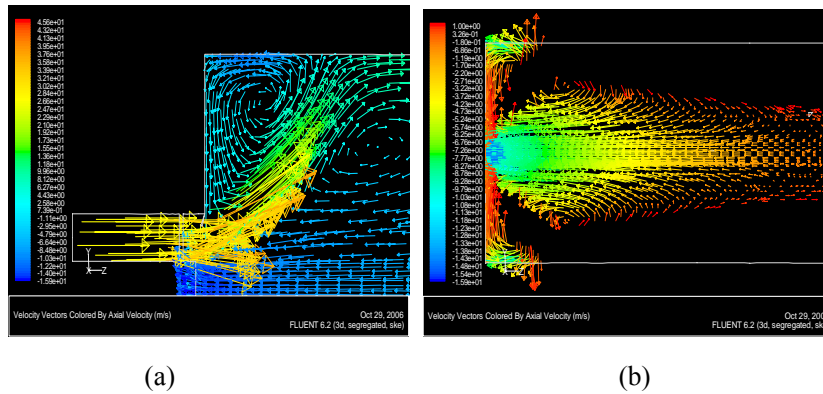

| (a) | (b) |

Figure 3: Velocity vector within the combustor (a) corner recirculation zone and (b) central recirculation zone (CRZ)

5.3   Inlet Flow Rate (Re$_D$)

Flow rate ranged from 0.025 kg/s to 0.105 kg/s (*Re$_D$* range is 26672 to 106690). Reynolds number can be calculated from mass flow rate as follows:

$$Re_D = \frac{\rho U D}{\mu} = \frac{4 \dot{m}}{\pi \mu D_h} \tag{9}$$

Swirler configuration with 8 vanes, r_o =23.9, r_i = 9.5 and 45° vane angle, is used to demonstrate the effect of mass flow rate (Reynolds number) on the flow filed within the combustor.

It can be observed from the negative axial velocity contours shown in Figure 4 that, there are vortices in the top and bottom corners enclosed by the jet coming out from the swirler exit. These corner vortices are shed from the dump plane. In addition a larger vortex (CRZ) is located around the combustor center line. Both vortices reverse the flow into the swirler exit direction.
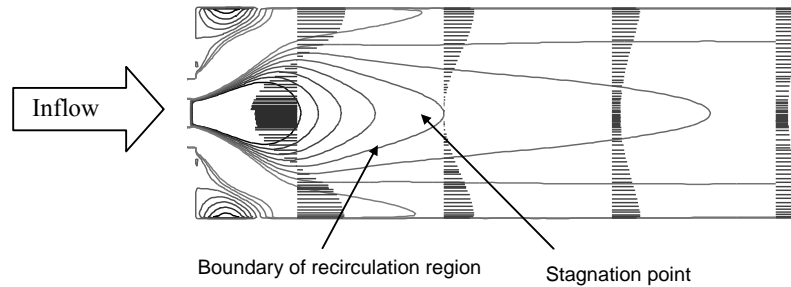
Figure 4: Profile of axial velocity within the combustor

Figures 5, 6 and 7 show the center-line mean axial and tangential velocity components, and turbulence intensity profile. Since the inlet mass flow rate increase, turbulence intensity, axial velocity tangential velocity components magnitudes increase within the central recirculation zone, as a result, the turbulence strength and recirculated gas quantity increase. Consequently, it can be concluded that the flame stability and mixing quality are improved with increasing inlet Reynolds number. However on the other side, the main flow jet velocity also increases with inlet mass flow consequently this may lead to flame blow off at excessive rate of inlet mass flow. Besides, the combustor pressure loss increases quadratically with increase of Re_D as shown in Figure 8.
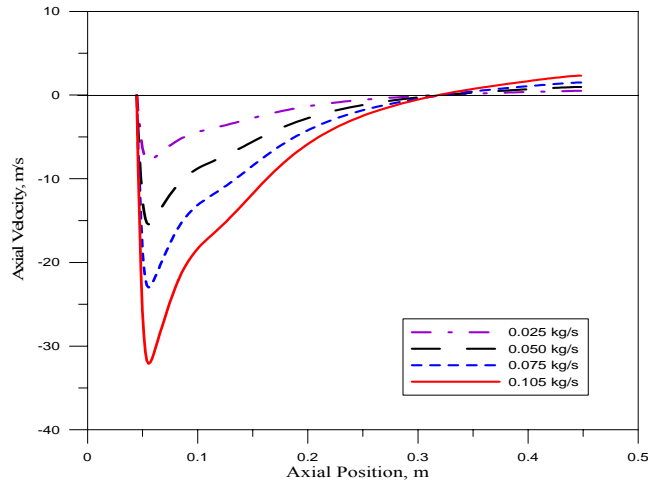
Figure 5: Mean axial velocity distributions along the combustor centerline
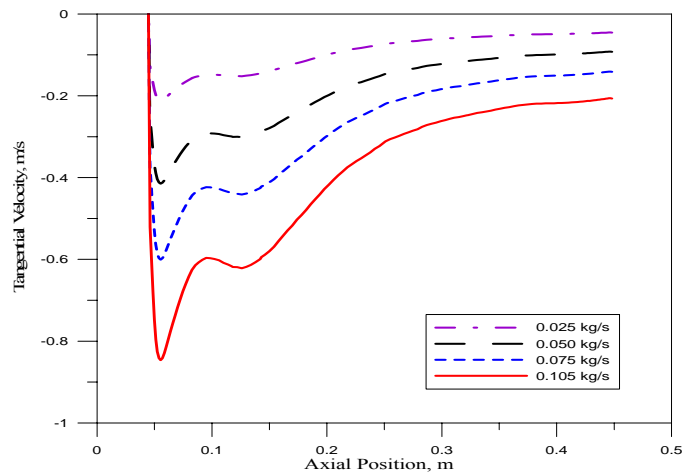
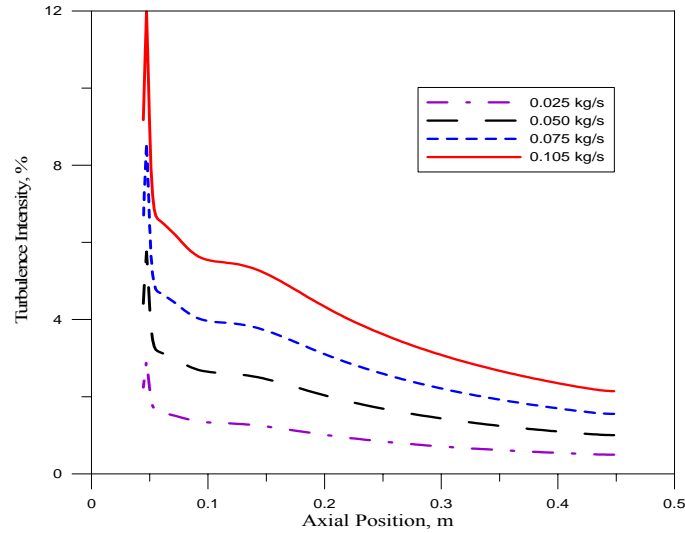Figure 6: Mean tangential velocity distributions along the combustor centerline

Figure 7: Turbulence intensity distributions along the combustor centerline
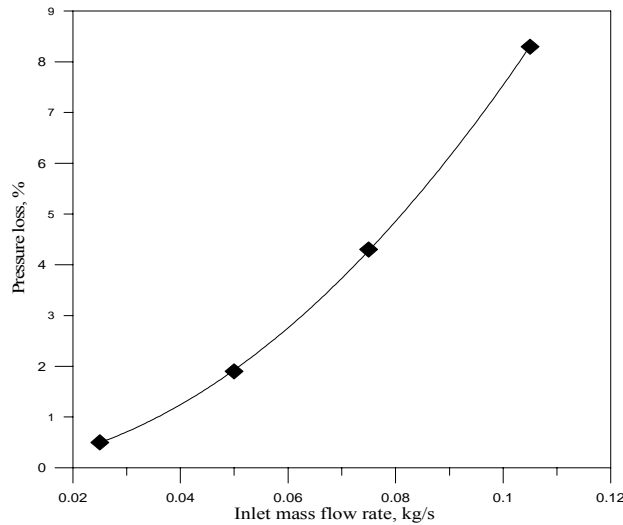

Figure 8: Pressure loss (%) versus inlet mass flow rate

5.4   Swirler Vane Number

Figures 9 and 10 depict the effect of varying the number of swirler vanes on the CRZ for swirler configuration of 45° blade angle with inlet mass flow 0.05 kg/s. Three swirlers with 8, 10 and 12 vanes were examined. Whereas the overall shape of outer border of the central recirculation zone doesn't change much. The 10 and 12-vanes swirlers produce higher turbulence intensity in the recirculation zone than for that 8-banes swirler. The results obtained for both 10 and 12 vanes swirlers are very close.
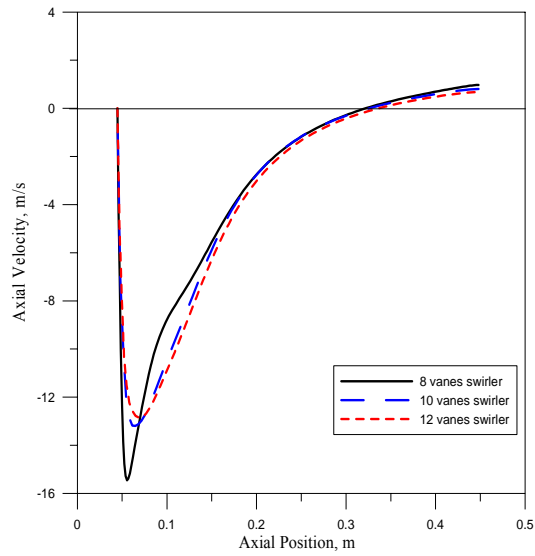
Figure 9: Mean axial velocity distributions along the centerline for
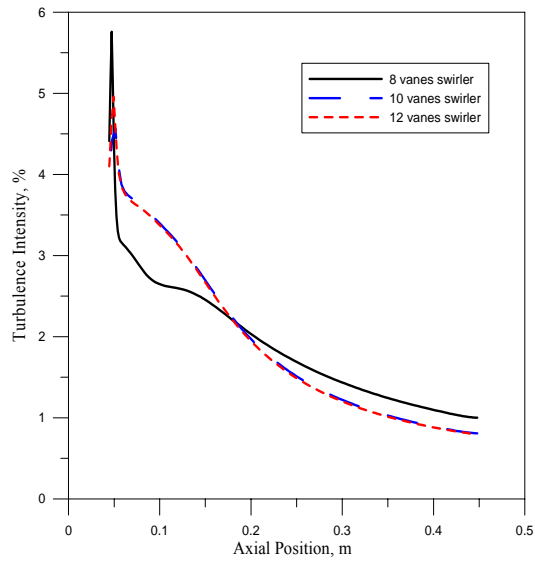different swirler vanes number

Figure 10: Turbulence intensity distributions along the centerline for
different swirler vanes number

5.5   Swirler Vane Angle

Three similar swirlers with different blade angles 30°, 45° and 60° which are corresponding to swirl number 0.43, 0.74, and 1.28 respectively were analyzed. It is shown from Figure 11 that the location of stagnation point was moved downstream with the increase in the swirler vane angle. Corresponding to this downwards movement of the stagnation point the strong rate-of-strain region on the centerline, which is formed by the shear layer between reversed flow and the recovered downwards flow, as well moved downstream. This indicates that the flame, which will be mainly anchored around the high strain rate region, will be pushed downstream with the increment of vane angle and more susceptible to blow off. In addition, when the vane angle increases, the maximum point of turbulence intensity moves upstream as the result it affects the air fuel mixing processes. This is due to highest turbulence region move towards the injector opening hole as the angle increases (Figure 12). Although increasing of the swirler vane angle enhances the recirculation zone, it significantly increases the pressure losses (Figure 13).
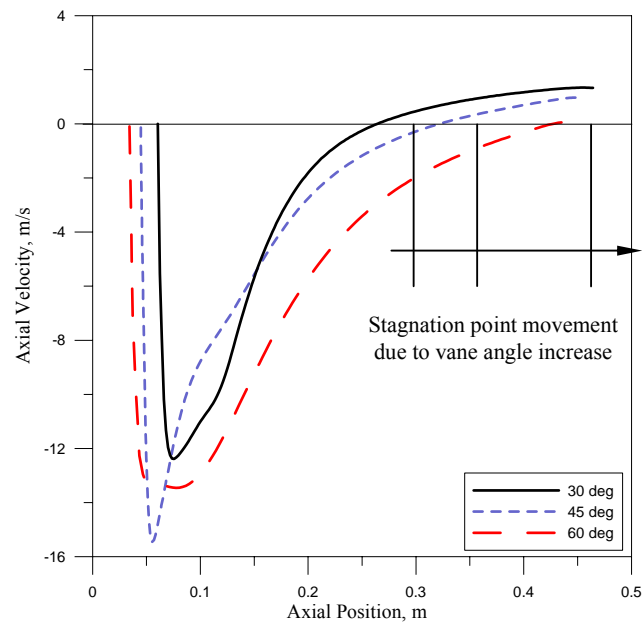

Figure 11: Mean axial velocity distributions along the centerline for different swirler vanes angle
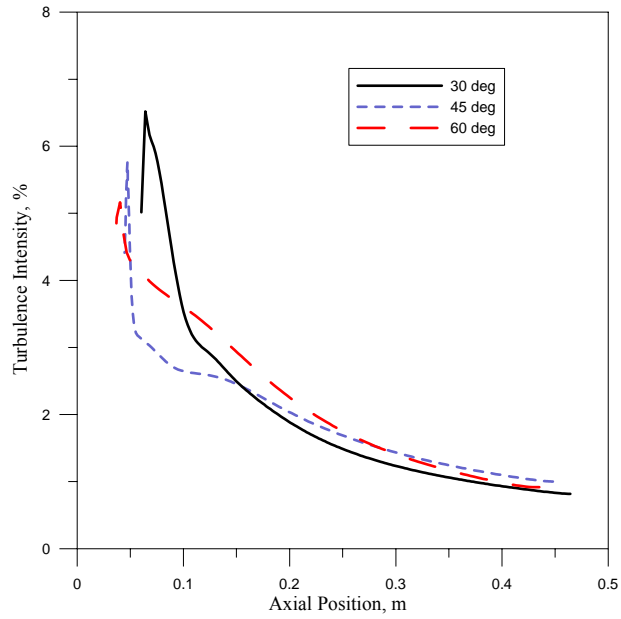
Figure 12: Turbulence intensity distributions along the centerline for
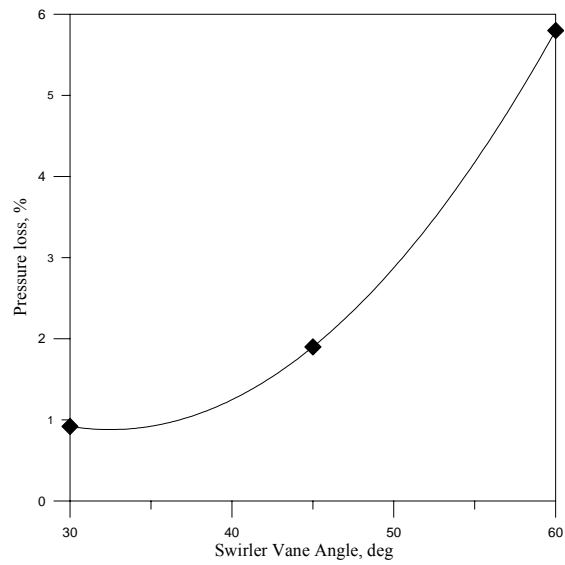different swirler vanes angle

Figure 13: Pressure loss % versus swirler vane angle

5.6   Confinement Ratio
Two confinement ratios (combustor diameter to swirler diameter ratio) of 3 (case A) and 2 (case B) are discussed to demonstrate the effect of swirler size on the flow dynamics inside the combustor. Figures 14 and 15 show the axial velocity and turbulence intensity along the combustor centre line. When the swirler area increases, the main flow velocity decreases. Therefore the turbulence strength and the quantity of the recirculating mass decreases. On the other hand, increasing the inlet area for the same mass flow decreases the pressure drop in the combustor.
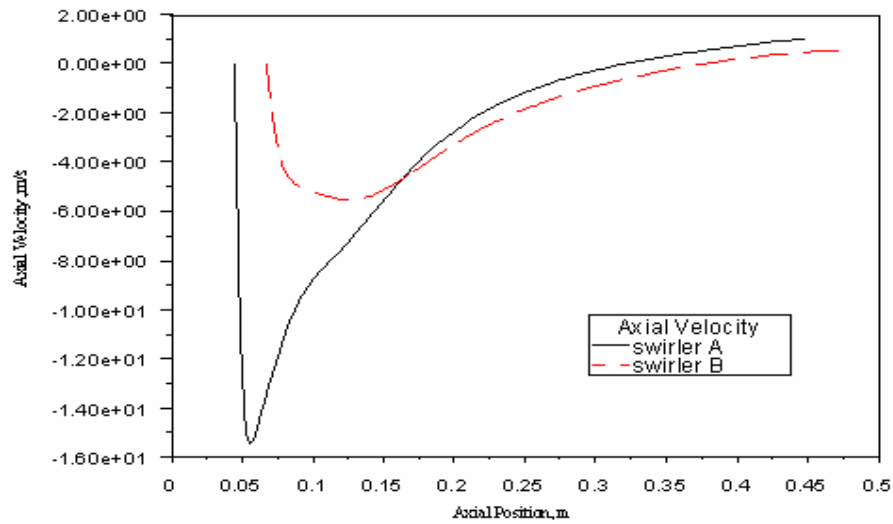

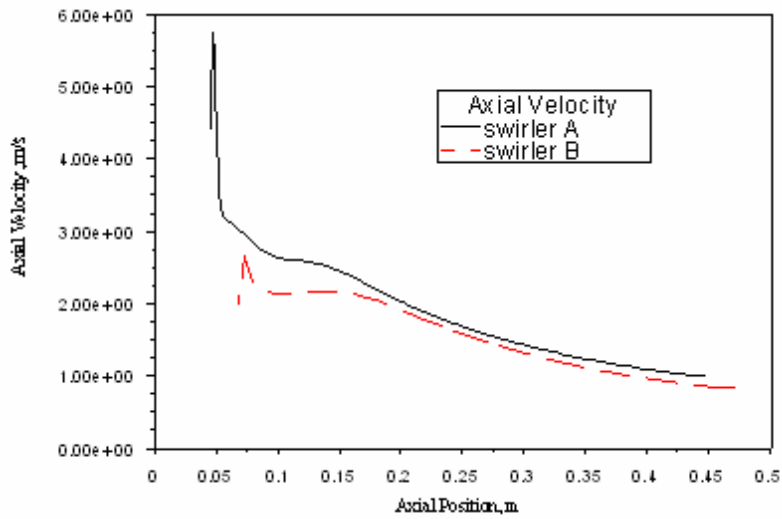Figure 14: Mean axial velocity distributions along the combustor centerline

Figure 15: Turbulence intensity distributions along the combustor centerline for different vanes number swirler

6.0   CONCLUSION

Air swirler is one of the most effective ways to induce flow recirculation inside the primary zone. This type of recirculation provides better mixing, In addition swirling flow is used to control the stability and intensity of the combustion and the size and shape of the flame region which is dependent on the size and shape of the recirculation zone.

It can be concluded from the previous discussion that the factors that have a significant effect on the size of the recirculation zone and turbulence inside primary zone are: mass flow rate, swirler vanes angle and confinement ratio. As the swirl number or Reynolds number increases, the length and the diameter of the central recirculation zone increases. As well as, the turbulence strength represented by the turbulence intensity increases as well as trapped mass in the recirculation bubble increases which can be expressed by the value of axial velocity and position of the stagnation point. On the other hand, the increase in the swirl number or Reynolds number results in more losses in the total pressure which will affect the combustion performances.

As observed from the analysis that have been done earlier, it can be concluded that at the highest value of swirl number ($S_N = 1.28$), it was able to produce the strongest circulation and highest recirculated mass flow inside the combustion chamber but on the contrary it has disadvantages of longest recirculation zone which makes the flame more susceptible to blow off and highest losses in total pressure..

Thus, It can also be concluded that, medium swirl number ($S_N = 0.74$) is the compromised solution between turbulence production and pressure losses.

ACKNOWLEDGEMENT

REFERENCES

1. Lefebvre, A.H., 1983. *Gas turbine combustion*, McGraw-Hill series.
2. Correa, S.M., 1993. A Review of NO_X Formation under Gas-Turbine Combustion Conditions, *Combustion Science and Technology*, Vol.87, 329-362.
3. Mellor, M., 1990. *Design of Modern Gas Turbine Combustors*, Academic Press.
4. Philip, P. Walsh and Fletcher, P., 2005. *Gas Turbine Performance*, Blackwell Science.
5. Wang, Y., Yang, V. and Yetter, R.A., 2004. *Numerical Study on Swirling Flow in an Cylindrical Chamber*, 42nd AIAA Aerospace Sciences Meeting, Reno, Nevada.

6. Karvinen and Ahlstedt, H., 2005. Comparison of Turbulence Models in Case of Jet in Cross Flow Using Commercial CFD Code, *Engineering Turbulence Modeling and Experiments 6*, Elsevier Ltd.

7. Menzies, K.R., 2005. An Evaluation of Turbulence Models for The Isothermal Flow in A Gas Turbine Combustion System, In *6th International Symposium on Engineering Turbulence Modeling and Experiments*, Sardinia, Italy.

8. Palma, J.M.L.M., 1988. Mixing in Non-Reacting Gas Turbine Combustor Flows, *Ph.D Thesis*, University of London, UK.

9. Hsiao, G. and Mongia, H., 2003. Swirl Cup Modeling Part III: Grid Independent Solution with Different Turbulence Models, *AIAA*.

10. Launder, B.N. and Spalding, D.B., 1972. *Lectures in Mathematical Models of Turbulence,* Academic Press, London, England.

11. Lin, S. and Griffiths, A.J., 1995. CFD simulation of cooling air flows within shrouded finned heater/cooler systems used on barrel extruders, *Proceedings of the Joint ASME/JSME Fluid Engineering Annual Conference*, USA.

12. FLUENT 6.2 User's Guide, Fluent Inc. 2005.

13. Versteeg, H.K. and Malalasekera, W., 1995. *An Introduction to Computational Fluid Dynamics, the Finite Volume Method*, Longman Group Ltd.